Physica Medica 55 (2018) 107–115

Contents lists available at ScienceDirect

Physica Medica

journal homepage: www.elsevier.com/locate/ejmp

Original paper

Dosimetric impact of Acuros XB dose-to-water and dose-to-medium reporting modes on VMAT planning for head and neck cancer

Carles Muñoz-Montplet[a,b,*], Jordi Marruecos[b,c], Maria Buxó[d], Diego Jurado-Bruggeman[a], Ingrid Romera-Martínez[a], Marta Bueno[e], Joan C. Vilanova[b,f]

[a] Medical Physics and Radiation Protection Department, Institut Català d'Oncologia, Avda. França s/n, 17007 Girona, Spain
[b] Department of Medical Sciences, University of Girona, C/Emili Grahit 77, 17003 Girona, Spain
[c] Radiation Oncology Department, Institut Català d'Oncologia, Avda. França s/n, 17007 Girona, Spain
[d] Girona Biomedical Research Institute (IDIBGI), Parc Hospitalari Martí i Julià, Edifici M2, Salt, 17190 Girona, Spain
[e] Laboratoire de dosimétrie des rayonnements ionisants, Institut de Radioprotection et de Sûreté Nucléaire, 31 Avenue de la Division Leclerc, 92260 Fontenay-aux-Roses, France
[f] Department of Radiology, Clínica Girona, Institut de Diagnòstic per la Imatge, C/Lorenzana 36, 17002 Girona, Spain

ARTICLE INFO

Keywords:
Acuros XB
Head and neck
VMAT
Dose-volume parameters

ABSTRACT

Purpose: To assess the dosimetric impact of switching from the Analytical Anisotropic Algorithm (AAA) to Acuros XB (AXB) for both dose-to-medium (Dm) and dose-to-water (Dw) in VMAT for H&N patients. To study whether it should be linked to a change in the dose prescriptions to the PTVs and in the constraints to the OARs.
Methods: 110H&N patients treated with VMAT were included. Calculations were performed with AAA and AXB. PTV54, PTV60, PTV70, spinal cord, brainstem, brain, larynx, oral cavity, cochleas, parotid glands and mandible were delineated. Clinically-relevant dose-volume parameters were compared. Paired t-tests were used to analyze the differences in mean values. The Pitman-Morgan dispersion test was computed to evaluate inter-patient variability of these differences.
Results: AAA overestimated all dose-volume parameters compared to AXB Dm (0.2 Gy to 2.4 Gy). No systematic trend was observed in the differences between AAA and AXB Dw (-5.3 Gy to 0.6 Gy). Dose-volume parameters were significantly higher for AXB Dw compared to AXB Dm (0.1 Gy to 6.6 Gy). In all cases, the largest absolute differences (4%–14%) were found for maximum absorbed doses to the cochleas and the mandible. The number of parameters with significant inter-patient variability was greater when switching from AAA to AXB Dw than from AAA to AXB Dm.
Conclusions: There are important differences between AXB and AAA in VMAT planning for H&N cancer. The systematic differences and their inter-patient variability identified may help to facilitate decision-making about the dose prescriptions to the PTVs and the constraints to the OAR.

1. Introduction

Volumetric modulated arc therapy (VMAT) has become increasingly common in recent years and appears to be slowly displacing static gantry intensity modulated radiation therapy (IMRT). The most common VMAT technique in head and neck (H&N) radiotherapy is dual arc simultaneous integrated boost (SIB) [1]. The H&N VMAT technique involves field segments that pass through areas of differing densities—air cavities, soft tissue, cartilage, and bone. Under these challenging dose calculation conditions, the Acuros XB (AXB) algorithm [2]—a grid-based linear Boltzmann transport equation solver implemented in the Eclipse treatment planning system (TPS)—has been shown to achieve accuracy rates comparable to Monte Carlo (MC) simulations, which is considered the most accurate dose calculation method in radiotherapy [3], and superior to the convolution/superposition algorithms used in routine clinical practice today. Numerous studies have compared AXB to measurements, MC, and convolution/superposition algorithms in water, in slab phantoms containing heterogeneities, and in anthropomorphic phantoms, for both simple fields and representative treatment planning setups [2,4–11].

* Corresponding author at: Medical Physics and Radiation Protection Department, Institut Català d'Oncologia, Avda. França s/n, 17007 Girona, Spain.
E-mail addresses: cmunoz@iconcologia.net (C. Muñoz-Montplet), jmarruecos@iconcologia.net (J. Marruecos), mbuxo@idibgi.org (M. Buxó), djurado@iconcologia.net (D. Jurado-Bruggeman), iromera@iconcologia.net (I. Romera-Martínez), marteta.3@gmail.com (M. Bueno), kvilanova@comg.cat (J.C. Vilanova).

https://doi.org/10.1016/j.ejmp.2018.10.024
Received 10 June 2018; Received in revised form 19 October 2018; Accepted 30 October 2018

The main advantage of the AXB algorithm is its accuracy. In addition, because the calculation times are only weakly dependent on the number of beams, AXB is a very efficient algorithm for VMAT even compared to the Analytical Anisotropic Algorithm (AAA) [8,12–14], a fast and widely-used convolution/superposition algorithm [15] that uses the same multiple-source model [16] as AXB. AXB calculates the energy-dependent electron fluence everywhere in the calculation volume. This enables both dose-to-medium (Dm) and dose-to-water (Dw) to be computed by using the corresponding energy deposition cross sections [2]. However, the optimal reporting mode (i.e, Dm vs. Dw) for clinical practice is not yet clear [3,17,18] and this debate is beyond the scope of this paper. Nonetheless, it is necessary to choose one of these reporting modes if the AXB algorithm is used.

Because both AXB and AAA algorithms are implemented in Eclipse, comparing them is relatively straightforward. Numerous studies have assessed the implications of using AXB for clinical dosimetry and their potential impact on clinical outcomes. Several of these studies have specifically examined how AXB impacts H&N treatment planning [8–10,19,20] while others have included only a subgroup of H&N patients as part of a more general evaluation of this algorithm [21,22]. Despite the availability of the aforementioned studies in H&N cancers, all of these studies present the same drawbacks: small sample sizes and a limited number of dose-volume parameters. Consequently, the statistical significance of the findings of those studies with regard to systematic differences between the compared algorithms is limited. Moreover, none of these studies has provided a statistical test to evaluate the inter-patient variability in the distribution of such differences, a key aspect that must be considered before switching to AXB for clinical use. Finally, several of those studies evaluated an older version of AXB (version 10) [9,10,19,21], which differs in many respects from more recent versions, most importantly with regard to CT-to-material conversions [23,24].

In this context, the aim of the present study was to assess the dosimetric impact of using AXB instead of AAA for AXB Dm and Dw reporting modes. Specifically, we examined whether moving from AAA to AXB should be linked to a change in the dose prescription and dose-volume reporting to the planning target volumes (PTV) and in constraints for organs at risk (OAR) in a large cohort of H&N patients. Here we report our findings on the systematic differences between these algorithms and their inter-patient variability for a wide range of dose-volume parameters in this cohort and we warn about the limitations on establishing universal recommendations for dose prescription as differences obtained between Dm and Dw will depend on the structures contained in the PTVs of the patient in particular.

2. Material and methods

2.1. Patient selection, contouring and prescription

The study population included 110 patients diagnosed with H&N cancer (oral cavity, larynx, oropharynx, nasopharynx, or hypopharynx) and treated with dual-arc VMAT at our institution between October 2013 and May 2015. The CT scans were performed with a GE Optima CT580 W CT Scanner (GE Healthcare, Chicago, IL, USA). Slice thickness was 2.5 mm. A QFIX Curve board (Qfix; Avondale, PA, USA) and a thermoplastic head and shoulder mask were used for immobilization.

Conventional or accelerated SIB was delivered in 33 or 35 fractions using a Clinac iX accelerator (Varian Medical Systems; Palo Alto, CA, USA). The PTV54, PTV60 and PTV70 (receiving 54, 60 and 70 Gy, respectively) were delineated by the radiation oncologist to encompass the tumour plus the at-risk nodal regions, the tumour and high risk nodal regions, and the tumour alone [25–28]. GTV-to-CTV and CTV-to-PTV isotropic margins were 0.5 cm. The following OARs were contoured in accordance with international guidelines: spinal cord, brainstem, brain, larynx, the oral cavity as a surrogate for the oral mucosa, cochleas, parotid glands, and mandible [26,29].

2.2. Treatment planning and dose calculation

Plans were created for a 6 MV photon beam with a Millennium 120 multileaf collimator (MLC) using RapidArc VMAT technique in the Eclipse TPS, version 13.0.33 (Varian Medical Systems; Palo Alto, CA, USA). All plans had two complete arcs.

The VMAT was optimized using the Progressive Resolution Optimizer of RapidArc until the plan was clinically acceptable according to the following criteria: 1) minimum dose (Dmin) to the PTVs $\geq$ 95% of the prescription dose; 2) maximum dose (Dmax) $\leq$ 107%; 3) maximum dose to the spinal cord and brainstem $<$ 45 Gy and 50 Gy, respectively; volume of brain receiving 60 Gy $<$ 1 cc; and mean doses to the oral cavity and parotid glands $\leq$ 35 Gy and 25 Gy, respectively.

Dose calculations were performed with the AAA and AXB (Dw and Dm) algorithms for the same number of monitor units, with identical beam and MLC setup. Calculation grid resolution was set to 2 mm in all cases. The same version (13.0.26) of AAA and AXB was used. Note that version 11 of AXB introduced an important change from version 10 with regard to the determination of tissue types from CT images [23,24]. AXB needs the macroscopic cross-section in each element of the computational grid. Eclipse provides AXB with a mass density and material type in each voxel of the image grid. In version 11 and above, if the mass density derived from the Hounsfield Units (HU) is within the range of two materials that are used in automatic CT to material conversion, then a linear mixture of these two materials is assigned to the voxel as shown in Fig. 1. It is important to note this difference because the version of AXB used in this study could assign different material compositions and thus produce different results than those previously obtained in studies that used version 10 [9,10,19].

2.3. Dose-volume parameters

Dose-volume histograms (DVH) were obtained using the Eclipse scripting API and exported to MATLAB (The Mathworks, Natick, MA, USA) to obtain the desired parameters for the PTVs and OARs for all patients.

ICRU report No. 83 [30] provides the data needed to harmonize prescribing, recording, and reporting of IMRT. The QUANTEC reviews [31] provide focused summaries of the dose/volume/outcome information for many organs.

The ICRU 83 recommended parameters were compared: near minimum absorbed dose D98, D95, median absorbed dose D50, and near maximum absorbed dose D2 to all PTVs, and homogeneity index [HI] = (D2-D98)/D50 for PTV70, where DX is the dose covering X% volumes.

Parameters collected in the QUANTEC reviews and other clinically-relevant dose-volume data for the OARs were compared: 1) Dmax to the spinal cord, brainstem, brain, cochleas and mandible; 2) Dmean for brain and larynx; and 3) Dmean to the oral cavity and parotid glands. D2 was also reported as an alternative to Dmax in the spirit of ICRU 83. Vx type parameters were discarded because they would have introduced biases in those cases in which the volume covered was 100% for all the algorithms and reporting modes.

2.4. Data analysis

Mean values, standard deviation (SD) and range (min–max) of the dose-volume parameters were calculated for each sample. Paired t-tests were used to analyze the differences in mean values between AAA and AXB Dm, AAA and AXB Dw, and AXB Dw and AXB Dm. Mean differences and 95% confidence intervals (CI) were also reported using the Statistical Package for Social Sciences, version 24 (IBM-SPSS, Chicago, IL).

To determine whether universal recommendations can be given for the treatment prescription when switching from AAA to AXB, it is

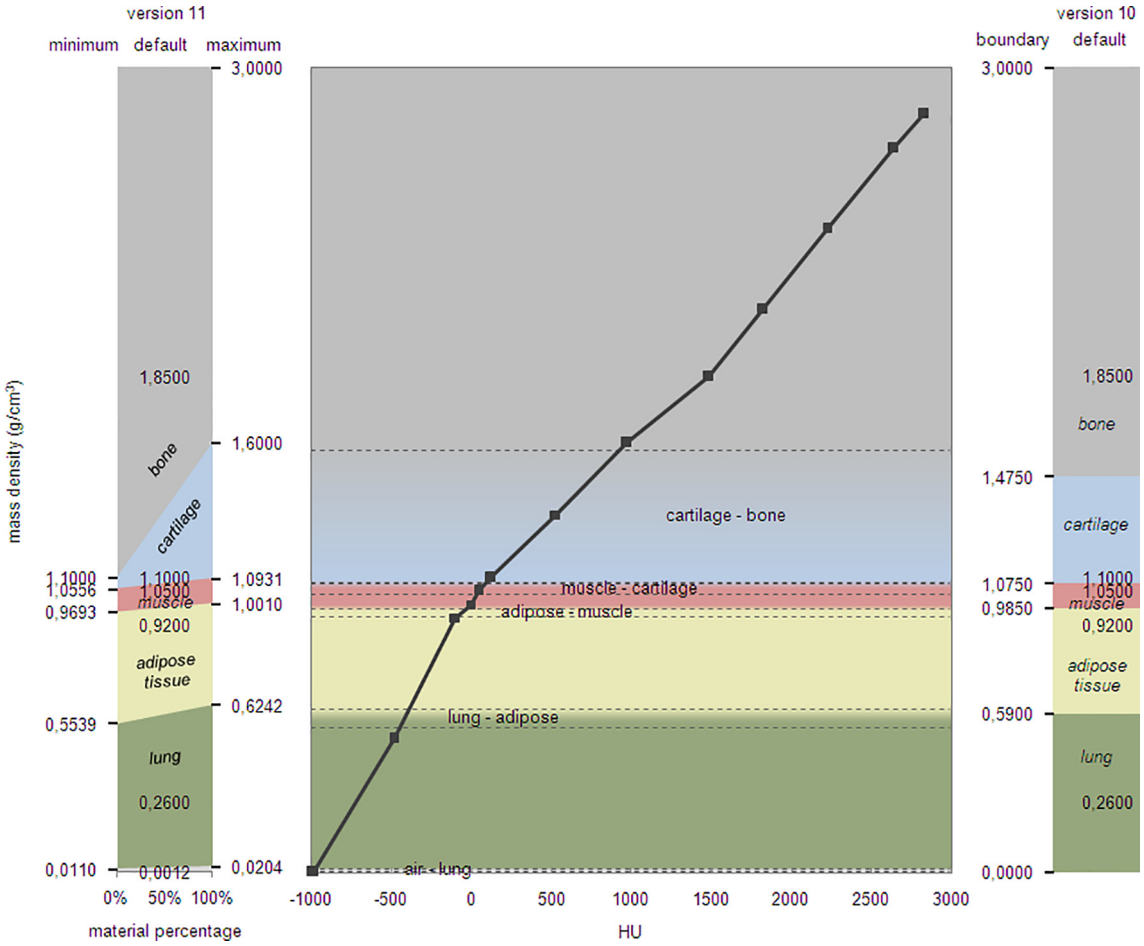

Fig. 1. Default HU-to-density calibration curve and graphic representation of density-to-material conversion tables versions 10 and 11. Each material is depicted by a color. In version 11, the overlapping region is represented by the ascending line separating the two materials, and for a given density the resulting composition is obtained by the relative amount of each material on both sides of the line.

necessary to know if these differences remain constant across all patients. For this purpose, the Pitman-Morgan dispersion test was computed using the R software, version 3.4.2 (R Core Team, 2017. R: A language and environment for statistical computing. R Foundation for Statistical Computing, Vienna, Austria.). The test determined if the ratios of the variances of each dose-volume parameter distributions were equal to one, comparing AAA and AXB Dm, AAA and AXB Dw, and AXB Dw and AXB Dm.

Both central tendency and dispersion tests were two-sided. P values < 0.05 were considered statistically significant.

According to the proposed methodology, two scenarios can be identified when switching from AAA to AXB (Dw or Dm) to help decision-making:

a) Inter-patient variability in a dose-volume parameter is non-significant: the related dose prescription parameter or constraint can be maintained or adjusted using a simple conversion factor depending on the significance of the systematic difference between the two algorithms.
b) Inter-patient variability in a dose-volume parameter is significant: AXB is not a simply scaled version of AAA in this case. No simple recommendations can be made.

Kernel densities for each algorithm and individual patient differences between AAA and AXB Dm, AAA and AXB Dw, and AXB Dw and AXB Dm were plotted for D50 to PTV70 and Dmax to the mandible as representative examples. Density plot is a variation of a histogram that uses kernel smoothing to plot values, allowing for smoother distributions by smoothing out the noise. An advantage density plots have over histograms is that they are better at determining the distribution shape because they are not affected by the number of bins used.

3. Results

Table 1 summarizes the mean, SD, and range of the PTVs and OAR dose-volume parameters across the 110 patients for the AAA, AXB Dm and AXB Dw algorithms. It also shows the statistical significance of the differences between the mean values and between the variances in the samples. Fig. 2 completes this information by graphically depicting the mean differences with 95% CIs.

Fig. 3a shows that differences in the mean values of D50 to PTV70 are statistically different (*t* test) from 0 except for AAA-AXB Dw ($p = 0.525$), which is reflected in the graph as fluctuations in the individual differences around the horizontal axis. Fig. 3b complements this information, showing the similarity of the variances identified by the Pitman-Morgan test. Fig. 3c shows that the ratio of the variances of Dmax to the mandible is statistically different (Pitman-Morgan test) from 1 except for AAA-AXB Dm ($p = 0.348$), which is reflected as a small inter-patient variability. The difference in the variances is due to the widening of the distribution for AXB Dw (Fig. 3d).

3.1. AAA versus AXB Dm

Fig. 2a shows that AAA statistically overestimated all dose-volume

Table 1
Descriptive statistics of PTVs and OARs dose-volume parameters and statistical significance of central tendency and dispersion differences over the whole sample.

	AAA			AXB Dm			AXB Dw			AAA-AXB Dm		AAA-AXB Dw		AXB Dw-AXB Dm	
	Mean ± SD	Min	Max	Mean ± SD	Min	Max	Mean ± SD	Min	Max	p-value *	p-value †	p-value *	p-value †	p-value *	p-value †
PTV54															
D98 (Gy)	50.60 ± 1.12	44.66	52.51	49.79 ± 1.15	43.42	51.70	50.48 ± 1.20	44.19	52.71	< 0.001	0.383	< 0.001	0.006	< 0.001	0.229
D95 (Gy)	51.82 ± 0.95	48.38	55.82	50.95 ± 0.95	47.32	55.15	51.61 ± 1.04	47.93	56.55	< 0.001	0.925	< 0.001	0.001	< 0.001	0.004
D50 (Gy)	57.25 ± 3.18	53.72	69.90	56.30 ± 3.08	52.69	68.78	57.11 ± 3.34	52.99	70.14	< 0.001	< 0.001	< 0.001	< 0.001	< 0.001	< 0.001
D2 (Gy)	72.02 ± 0.74	69.84	74.43	70.90 ± 0.77	68.61	73.30	72.29 ± 0.94	69.67	75.19	< 0.001	0.229	< 0.001	< 0.001	< 0.001	< 0.001
PTV60															
D98 (Gy)	57.97 ± 1.46	52.36	60.90	56.94 ± 1.30	52.80	60.05	58.00 ± 1.36	53.94	61.25	< 0.001	0.013	0.727	0.127	< 0.001	0.293
D95 (Gy)	59.48 ± 1.37	55.86	64.04	58.35 ± 1.40	55.40	63.95	59.40 ± 1.52	56.22	65.12	< 0.001	0.245	0.043	< 0.001	< 0.001	0.007
D50 (Gy)	68.01 ± 2.00	61.49	70.70	66.84 ± 1.97	60.31	69.58	68.05 ± 2.03	61.46	70.64	< 0.001	0.068	0.205	0.259	< 0.001	0.024
D2 (Gy)	72.58 ± 0.69	71.01	75.18	71.53 ± 0.69	70.06	73.99	73.26 ± 1.28	71.58	79.45	< 0.001	0.757	< 0.001	< 0.001	< 0.001	< 0.001
PTV70															
D98 (Gy)	65.42 ± 2.56	50.00	68.13	64.30 ± 2.06	51.40	66.90	65.63 ± 2.11	52.41	68.47	< 0.001	< 0.001	0.020	< 0.001	< 0.001	0.514
D95 (Gy)	66.67 ± 1.24	59.90	68.71	65.49 ± 1.13	59.15	67.50	66.78 ± 1.05	60.83	68.86	< 0.001	0.016	0.036	< 0.001	< 0.001	0.210
D50 (Gy)	70.17 ± 0.49	68.88	71.48	68.97 ± 0.48	67.76	70.22	70.15 ± 0.52	69.27	71.84	< 0.001	0.770	0.525	0.320	< 0.001	0.208
D2 (Gy)	72.77 ± 0.70	71.48	75.85	71.78 ± 0.68	70.55	74.61	73.65 ± 1.45	71.79	81.60	< 0.001	0.406	< 0.001	< 0.001	< 0.001	< 0.001
HI	0.10 ± 0.04	0.05	0.33	0.11 ± 0.03	0.06	0.29	0.11 ± 0.04	0.07	0.34	0.006	< 0.001	< 0.001	0.849	0.005	0.004
Spinal cord															
Dmax (Gy)	47.69 ± 2.34	38.75	53.20	46.54 ± 2.21	38.40	51.93	47.96 ± 2.22	39.45	53.20	< 0.001	0.021	< 0.001	0.028	< 0.001	0.875
D2 (Gy)	43.65 ± 2.24	36.12	49.12	42.58 ± 2.11	35.69	47.70	43.47 ± 2.17	36.37	48.68	< 0.001	< 0.001	< 0.001	< 0.001	< 0.001	< 0.001
Brainstem															
Dmax (Gy)	44.95 ± 6.75	5.40	53.05	43.94 ± 6.53	4.90	51.75	44.84 ± 6.72	5.00	53.49	< 0.001	< 0.001	0.138	0.684	< 0.001	< 0.001
D2 (Gy)	41.31 ± 7.10	5.17	49.75	40.32 ± 6.91	4.60	48.33	40.98 ± 7.03	4.68	49.02	< 0.001	< 0.001	< 0.001	0.011	< 0.001	< 0.001
Brain															
Dmax (Gy)	52.87 ± 10.36	21.85	74.05	52.24 ± 10.32	21.40	73.80	54.10 ± 10.83	22.25	76.40	< 0.001	0.388	< 0.001	< 0.001	< 0.001	< 0.001
D2 (Gy)	33.26 ± 10.59	6.39	64.63	32.57 ± 10.43	6.05	64.00	33.19 ± 10.62	6.15	65.08	< 0.001	< 0.001	< 0.001	0.063	< 0.001	< 0.001
Dmean (Gy)	5.15 ± 2.76	1.07	17.10	4.96 ± 2.68	1.01	16.65	5.05 ± 2.73	1.03	16.94	< 0.001	< 0.001	< 0.001	< 0.001	< 0.001	< 0.001
Larynx															
Dmean (Gy)	50.45 ± 15.23	0.98	72.01	49.27 ± 15.16	0.74	70.43	49.93 ± 15.41	0.74	71.99	< 0.001	0.003	< 0.001	< 0.001	< 0.001	< 0.001
Oral cavity															
Dmean (Gy)	37.17 ± 12.13	4.12	70.31	36.51 ± 12.13	4.04	69.08	37.51 ± 12.33	4.15	70.35	< 0.001	0.910	< 0.001	0.006	< 0.001	0.017
Left cochlea															
Dmax (Gy)	24.44 ± 16.95	1.95	71.00	22.88 ± 16.04	1.75	67.35	25.87 ± 18.22	1.90	77.30	< 0.001	< 0.001	< 0.001	< 0.001	< 0.001	< 0.001
D2 (Gy)	23.14 ± 16.25	1.02	70.57	21.61 ± 15.32	0.53	66.87	24.47 ± 17.49	0.74	76.56	< 0.001	< 0.001	< 0.001	< 0.001	< 0.001	< 0.001
Right cochlea															
Dmax (Gy)	25.15 ± 16.31	1.80	66.45	23.47 ± 15.41	1.65	63.00	26.69 ± 17.56	1.75	72.45	< 0.001	< 0.001	< 0.001	< 0.001	< 0.001	< 0.001
D2 (Gy)	23.82 ± 15.64	0.49	66.15	22.16 ± 14.83	0.25	62.67	25.22 ± 16.83	0.23	71.87	< 0.001	< 0.001	< 0.001	< 0.001	< 0.001	< 0.001
Left parotid															
Dmean (Gy)	26.44 ± 8.71	16.16	70.03	25.49 ± 8.61	16.03	68.29	25.83 ± 8.78	16.19	69.56	< 0.001	< 0.001	< 0.001	0.005	< 0.001	< 0.001
Right parotid															
Dmean (Gy)	28.16 ± 10.03	9.44	64.75	27.22 ± 10.01	9.24	63.25	27.58 ± 10.13	9.36	64.39	< 0.001	0.367	< 0.001	< 0.001	< 0.001	< 0.001
Mandible															
Dmax (Gy)	67.30 ± 7.65	47.10	76.00	65,98 ± 7.60	46.00	75.60	72.61 ± 10.53	49.05	100.08	< 0.001	0.529	< 0.001	< 0.001	< 0.001	< 0.001
D2 (Gy)	62.61 ± 9.20	39.40	74.18	60.23 ± 9.00	33.70	71.25	65.95 ± 10.24	36.80	82.70	< 0.001	< 0.001	< 0.001	< 0.001	< 0.001	< 0.001

* : central tendency; † : dispersión

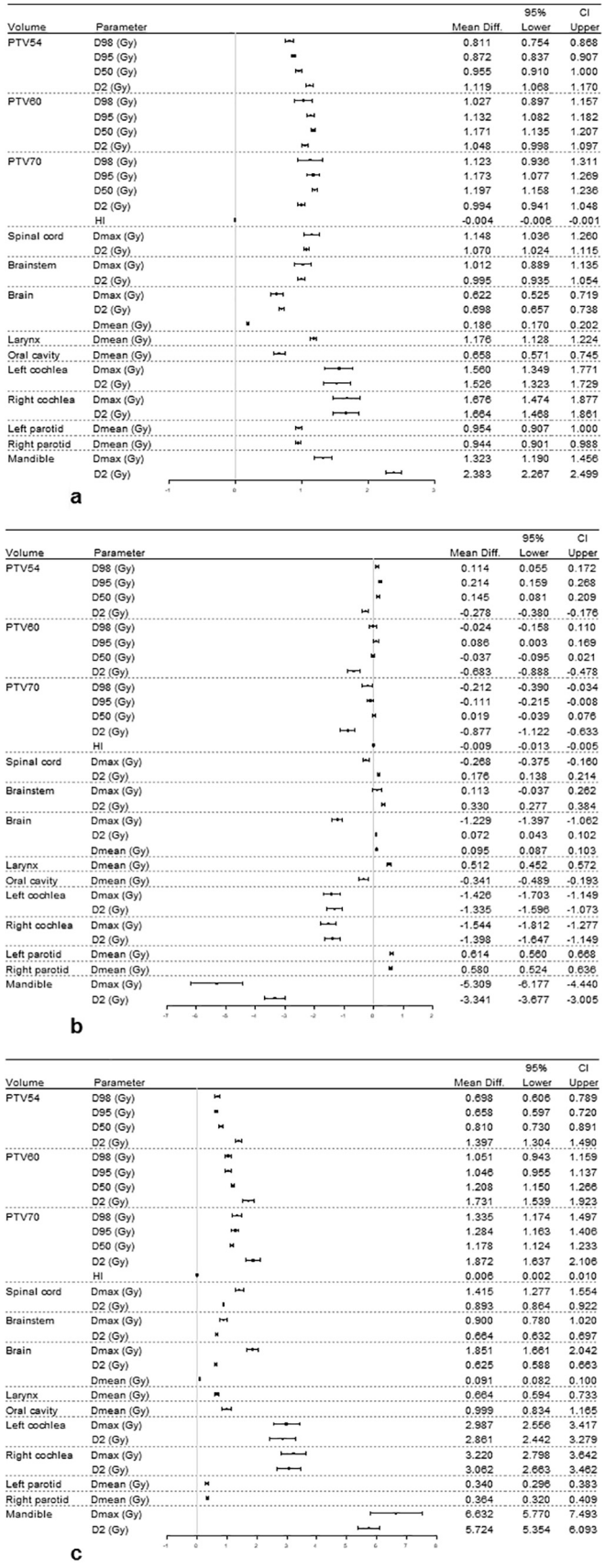

Fig. 2. Mean differences and 95% CI of the dose-volume parameters to the PTV and OARs for the whole sample for (a) AAA-AXB Dm, (b) AAA-AXB Dw, and (c) AXB Dw-AXB Dm.

parameters compared to AXB Dm.

Regarding the PTVs, the dose increase calculated by AAA was similar for all dose-volume parameters, with a mean of 1.05 Gy (1.7%). The HI of PTV70 predicted by AAA was 4% lower than the HI obtained with AXB Dm. Dispersion among patients was not significant (Table 1) except for the coverage represented by D98 to PTV60 and PTV70, for D95 to PTV70, for median dose D50 to PTV54, and for the HI.

The largest absolute difference between the two algorithms for OARs was observed in the D2 to the mandible (2.38 Gy, 4.0%). The largest percentage differences were found for the parameters of the cochleas, ranging from 6.8% (1.56 Gy) for Dmax to the left cochlea to 7.5% (1.66 Gy) for D2 to the right cochlea. There was a significant inter-patient variability in most cases, except for Dmax to the brain and mandible and Dmean to the oral cavity and the right parotid.

3.2. AAA versus AXB Dw

As Fig. 2b shows, no systematic trend in the differences between the two algorithms was observed.

The PTV values obtained by both algorithms were similar, with the largest difference being the D2 to PTV70 (−0.88 Gy, −1.2%). The HI calculated by AAA was 8% lower than the AXB Dw HI. Differences in D98 and D50 to PTV60 and D50 to PTV70 were not significant. Inter-patient variability was significant except for D98 and D50 to PTV60, and D50 to PTV70 and the HI.

The largest differences between the AAA and AXB Dw algorithms for OARs were observed in the mandible and the cochleas, similar to the comparison described above for AXB Dm. Specifically, Dmax to the mandible and Dmax to the right cochlea predicted by AAA were 5.31 Gy (7.3%) and 1.54 Gy (5.8%) lower than those predicted by AXB Dw. For the other organs and parameters, the differences were < 1.23 Gy or 2.4%. All differences were statistically significant except for Dmax to the brainstem. Variability among patients was also significant except for Dmax to the brainstem and D2 to the brain.

3.3. AXB Dw vs AXB Dm

All dose-volume parameters were significantly higher (Fig. 2c) for AXB Dw compared to AXB Dm.

For the PTVs, the dose increase when using AXB Dw was similar for all dose-volume parameters, with an average of 1.19 Gy (1.9%). The HI of PTV70 reported in the medium was 5.5% lower than in water. Inter-patient variability was significant, except for D95 and D50 to PTV70 and for D98 to all the PTVs.

As in the previous comparisons, the largest differences for the OARs were found for the cochleas and the mandible. Both D2 and Dmax to the cochleas and mandible calculated with AXB Dw were, respectively, approximately 3 Gy (13%–14%) and 6 Gy (9%–10%) higher than those obtained with AXB Dm. Differences for the other OARs were smaller, with the most notable being the brain Dmax (1.86 Gy, 3.6%). Dispersion was significantly different between the two reporting modes, except for Dmax to the spinal cord.

Table 2 summarizes the classification of the dose-volume parameters according to the significance of the two statistical tests when switching from AAA to AXB. Upper rows correspond to scenario a) while lower rows correspond to scenario b).

4. Discussion

The aim of this study was to evaluate the dosimetric impact of using the AXB versus the AAA algorithm in a large series of patients diagnosed with H&N cancer and treated with VMAT. Our main findings were as follows: 1) the AAA algorithm statistically overestimated all dose-volume parameters compared to AXB Dm, 2) no systematic trend was observed in the differences between AAA and AXB Dw, and 3) all dose-volume parameters were significantly higher for AXB Dw versus

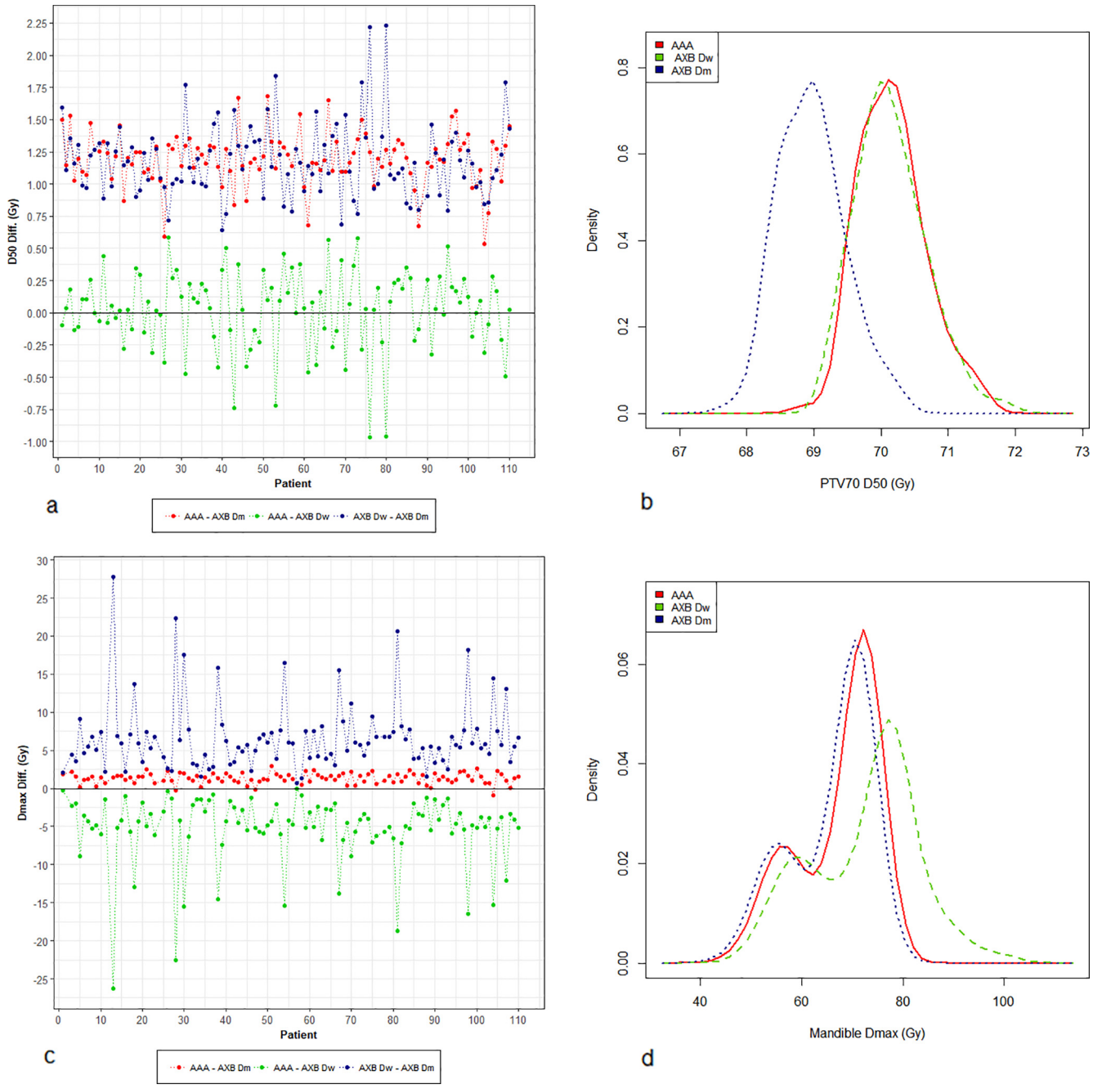

Fig. 3. (a) PTV70 D50 individual patient differences, (b) PTV70 D50 kernel density plots, (c) mandible Dmax individual patient differences, and (d) mandible Dmax kernel density plots.

AXB Dm. In all cases, the largest differences were found for the dose-volume parameters for the cochleas and the mandible. The number of parameters with significant inter-patient variability of the differences was greater when switching from AAA to AXB Dw than from AAA to AXB Dm.

To our knowledge, our study—which included 110 patients—is the largest to date to compare the AXB (Dm and Dw) and AAA algorithms in H&N patients treated with VMAT. Previous studies evaluated samples of up to 15 patients [9,10,19–22]. Moreover, they were all based on static gantry IMRT techniques [9,20,22], an older version (v. 10) of AXB [9,10,19,21], or presented results only for the Dm mode [9,19–21].

In terms of systematic differences, the AAA algorithm overestimated PTV dose-volume parameters compared to AXB Dm, a finding that is largely consistent with the results of the aforementioned studies. Published data on differences between the AAA and AXB algorithms with regards to dose-volume parameters to OARs in H&N are scant [9,19–22]. Only the study by Kathirvel et al. [21] evaluated the oral cavity, and only Kan et al. [19] included the mandible and the inner ear in their evaluation. Overall, our findings agree with published results and provide relevant additional information on dose-volume parameters for several OARs. It is interesting to point out that the magnitude of the systematic differences found between AAA and AXB Dm for both PTVs and OARs are close to the dosimetric changes in H&N plans due to linac composite miscalibration at general tolerance level [32].

Two previous studies have compared AXB Dw to AAA in H&N patients [10,22], with both studies finding that the mean doses to the PTVs were similar for the two algorithms, a finding that is consistent

Table 2
Classification of the dose-volume parameters according to the significance of the statistical tests when switching from AAA to (a) AXB Dm and to (b) AXB Dw.

AAA-AXB Dm		Dose-volume parameters systematic differences	
		Non-significant	Significant
Dose-volume parameters inter-patient variability	Non-significant	-	PTV54: D98, D95, D2 PTV60: D95, D50, D2 PTV70: D50, D2 Brain: Dmax Oral Cavity: Dmean Right parotid: Dmean Mandible: Dmax
	Significant	-	PTV54: D50 PTV60: D98 PTV70: D98, D95, HI Spinal cord: Dmax, D2 Brainstem: Dmax, D2 Brain: D2, Dmean Larynx: Dmean Left cochlea: Dmax, Dmean Right Cochlea: Dmax, Dmean Left parotid: Dmean Mandible: D2

(a)

AAA-AXB Dw		Dose-volume parameters systematic differences	
		Non-significant	Significant
Dose-volume parameters inter-patient variability	Non-significant	PTV60: D98, D50 PTV70: D50 Brainstem: Dmax	Brain: D2 PTV70: HI
	Significant	-	PTV54: D98, D95, D50, D2 PTV60: D95, D2 PTV70: D98, D95, D2 Spinal cord: Dmax, D2 Brainstem: D2 Brain: Dmax, Dmean Larynx: Dmean Oral Cavity: Dmean Left cochlea: Dmax, Dmean Right Cochlea: Dmax, Dmean Left parotid: Dmean Right parotid: Dmean Mandible: Dmax, D2

(b)

with our observations for D50. However, only the most recent of those studies (Zifodya et al.) [22] included OARs (spinal cord and parotid glands). The results of that study, in terms of systematic differences, were similar to ours. They also reported parameters for PTVs such as D98, D95 and D2, with the most notable result being that D2 was significantly higher when calculated with AXB Dw. Our results pointed on the same direction. We could correlate this effect to the random presence of portions of cartilage or bone in the PTVs.

For bone, when the AAA conventional photon dose calculation is performed using water with relative electron densities, this results in dose distributions that are much closer to Dm distributions than to Dw distributions converted using mass stopping-power ratios of water to bone [17]. This explains the observed systematic higher doses in volumes composed of high Z materials such as the cochleas or the mandible, and the "hot spots" in the PTVs containing bone or cartilage, that increase the average Dmax and D2, when the AXB Dw reporting mode was used compared to AXB Dm or AAA. Fig. 4 shows an example of a "hot spot" in a PTV containing bone. The opposite happens with the presence of air, but to a lesser extent. Several of the studies described above segmented the PTVs into subvolumes composed solely of soft tissue, air, bone or cartilage to quantify the systematic differences introduced when reporting the dose in water [10,19,20], but none did so for OARs.

The "hot spots" calculated by AXB Dw in some patients, i.e. with PTVs containing cartilage or bone and also, for example, with mandibles containing metallic implants, are random unidirectional effects across the entire group of patients that can lead to differences in the width of the distributions of the dose-volume parameters, preventing the formulation of universal recommendations for the PTV dose prescription and OAR constraints when switching from AAA to AXB. In order to objectively determine if the distribution variances of the algorithms were significantly different, we applied the Pitman-Morgan test, a tool that is used as a complement to the more widely-used statistical tests for central values. As expected, the Pitman-Morgan test predicted less inter-patient variability when switching from AAA to AXB Dm than when switching from AAA to AXB Dw (Table 2). To ensure a comprehensive comparison, the test was also used to compare the Dm and Dw reporting modes for AXB.

The results obtained in this study could facilitate decision-making when adopting AXB for head and neck VMAT treatments. For example, with respect to AAA, Dmax to the mandible would be approximately 1 Gy (2%) lower when using AXB Dm, and in addition this statement is reasonably applicable to all patients, so increased probability of complications is not expected if Dmax restrictions for the mandible are maintained or even decreased by a 2% when switching to AXB Dm. Another example regarding prescription is that D50 to PTV70 would be approximately the same for AAA and AXB Dw, and inter-patient variability is again non-significant, so it seems reasonable to keep the actual prescription dose if one opts for AXB Dw. These two examples correspond to scenario a).

Notwithstanding these results, it is important to emphasize that inter-patient variability is too high to establish simple recommendations for most parameters (scenario b)), even for AXB Dm. In these cases, further study is still required regarding the prediction of clinical outcomes from the dose-volumetric parameters calculated by AXB when they differ from the parameters calculated with AAA, on which current clinical knowledge is based. In our center, which AXB reporting mode to adopt is still a matter of debate. On one hand, our findings support the use of AXB Dm in terms of traceability to the convolution/superposition algorithms in the sense that the differences between the two are more systematic than for AXB Dw. On the other hand, AXB Dw might better predict clinical outcomes. Specifically, individual clinically relevant differences for the maximum doses to the mandible were obtained in a subgroup of patients. Our current research focuses on the predictive power of AAA, AXB Dm and AXB Dw for mandible osteonecrosis. This information, together with the advantages and disadvantages of using the Dw or Dm for reporting discussed in detail elsewhere [3,17,18], will help us make a decision. For this to be possible in H&N VMAT treatments, it is essential to implement a global strategy to better assess the dose delivered to the patients, including in-vivo dosimetry [33] and deformable image registration for daily dose calculation [34].

A limitation of the present work is the use of a single 2 mm calculation grid size. Smaller grid resolution reduces the averaging effect and leads to better sampling of the structure voxels to the calculation grid [9]. Moreover, the grid size also influences the relative dose difference between the AAA and AXB algorithms, which is the focus of our study. To our knowledge, the potential impact of the grid size on the dose difference between AAA and AXB has only been assessed for stereotactic and conventional lung VMAT plans [13,35]. Relative dose differences calculated with 2.5 mm and 1 mm grid sizes differed < 1% for all dose-volume parameters analyzed. Although we decided to choose

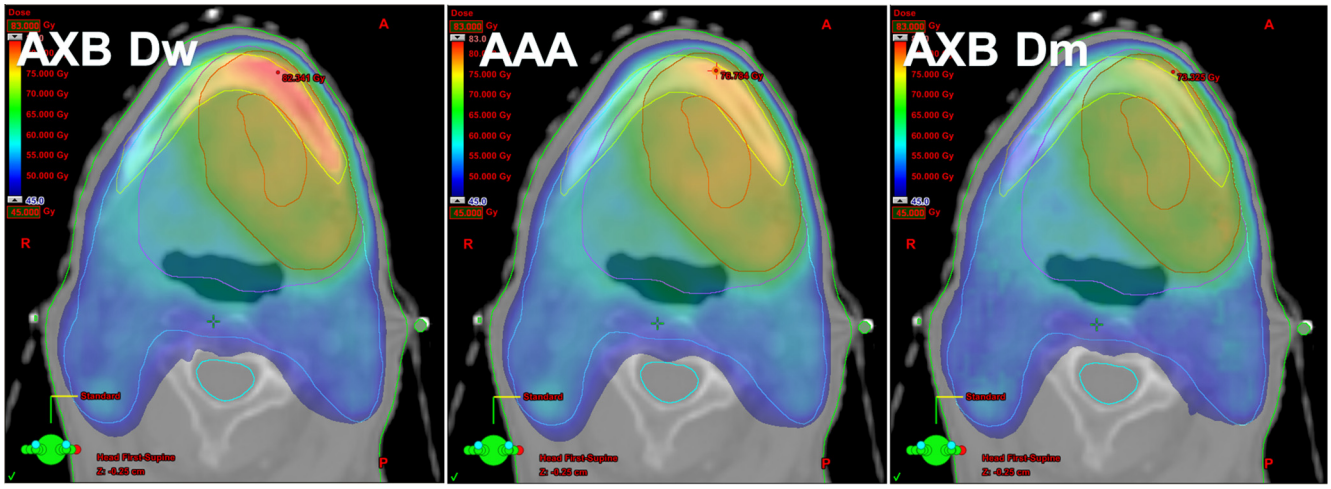

Fig. 4. A "hot spot" calculated by AXB in a PTV containing bone when dose is reported to water compared to AAA and AXB Dm. Dmax is 82.3 Gy, 76.8 Gy and 73.3 Gy for AXB Dw, AAA and AXB Dm respectively.

the resolution used in our clinical routine, the influence of smaller grid sizes will be another area of interest for us.

5. Conclusions

The present study shows that there are important differences between the AXB (for both the Dw and Dm reporting modes) and the AAA dose calculation algorithms in VMAT planning for H&N cancer patients. The systematic differences and their inter-patient variability in the dose-volume parameters between the AXB and AAA algorithms provide valuable information relative to the impact on the dose prescriptions to the PTVs and on the constraints to the OAR. These findings could facilitate decision-making at radiotherapy centers considering switching to the AXB algorithm for H&N VMAT treatments. However, further research is needed to better assess the predictive accuracy of the dose-volume parameters calculated by this algorithm for clinical outcomes.

Acknowledgements

The authors acknowledge fruitful discussions with Rafael Fuentes-Raspall and Núria Jornet and the help of Albert Onses with Matlab scripting. We thank Bradley Londres for professional English language editing.

Funding

This research did not receive any specific grant from funding agencies in the public, commercial, or not-for-profit sectors.

References

[1] Macchia G, Deodato F, Cilla S, Cammelli S, Guido A, Ferioli M, et al. Volumetric modulated arc therapy for treatment of solid tumors: Current insights. Onco Targets Ther 2017;10:3755–72. https://doi.org/10.2147/OTT.S113119.

[2] Vassiliev ON, Wareing TA, McGhee J, Failla G, Salehpour MR, Mourtada F. Validation of a new grid-based Boltzmann equation solver for dose calculation in radiotherapy with photon beams. Phys Med Biol 2010;55:581–98. https://doi.org/10.1088/0031-9155/55/3/002.

[3] Chetty IJ, Curran B, Cygler JE, DeMarco JJ, Ezzell G, Faddegon BA, et al. Report of the AAPM Task Group No. 105: Issues associated with clinical implementation of Monte Carlo-based photon and electron external beam treatment planning. Med Phys 2007;34:4818–53. https://doi.org/10.1118/1.2795842.

[4] Fogliata A, Nicolini G, Clivio A, Vanetti E, Mancosu P, Cozzi L. Dosimetric validation of the Acuros XB advanced dose calculation algorithm: fundamental characterization in water. Phys Med Biol 2011;56:1879–904. https://doi.org/10.1088/0031-9155/56/6/022.

[5] Fogliata A, Nicolini G, Clivio A, Vanetti E, Cozzi L. Dosimetric evaluation of Acuros XB Advanced Dose Calculation algorithm in heterogeneous media. Radiat Oncol 2011;6:82. https://doi.org/10.1186/1748-717X-6-82.

[6] Bush K, Gagne IM, Zavgorodni S, Ansbacher W, Beckham W. Dosimetric validation of Acuros® XB with Monte Carlo methods for photon dose calculations. Med Phys 2011;38:2208–21. https://doi.org/10.1118/1.3567146.

[7] Han T, Mikell J, Salehpour M, Mourtada F. MO-F-BRB-02: dosimetric comparison of Acuros XB deterministic radiation transport method with monte carlo and model-based convolution methods in heterogeneous media. Med Phys 2011;38:3722. https://doi.org/10.1118/1.3613003.

[8] Han T, Mourtada F, Kisling K, Mikell J, Followill D, Howell R. Experimental validation of deterministic Acuros XB algorithm for IMRT and VMAT dose calculations with the Radiological Physics Center's head and neck phantom. Med Phys 2012;39:2193–202. https://doi.org/10.1118/1.3692180.

[9] Kan MWK, Leung LHT, Yu PKN. Verification and dosimetric impact of Acuros XB algorithm on intensity modulated stereotactic radiotherapy for locally persistent nasopharyngeal carcinoma. Med Phys 2012;39:4705–14. https://doi.org/10.1118/1.4736819.

[10] Kan MWK, Leung LHT, So RWK, Yu PKN. Experimental verification of the Acuros XB and AAA dose calculation adjacent to heterogeneous media for IMRT and RapidArc of nasopharyngeal carcinoma. Med Phys 2013;40:1–19. https://doi.org/10.1118/1.4792308.

[11] Lloyd SAM, Ansbacher W. Evaluation of an analytic linear Boltzmann transport equation solver for high-density inhomogeneities Evaluation of an analytic linear Boltzmann transport equation solver for high-density inhomogeneities 2013; 011707: 3–7. doi: 10.1118/1.4769419.

[12] Fogliata A, Nicolini G, Clivio A, Vanetti E, Cozzi L. Critical appraisal of acuros XB and anisotropic analytic algorithm dose calculation in advanced non-small-cell lung cancer treatments. Int J Radiat Oncol Biol Phys 2012;83:1587–95. https://doi.org/10.1016/j.ijrobp.2011.10.078.

[13] Kroon PS, Hol S, Essers M. Dosimetric accuracy and clinical quality of Acuros XB and AAA dose calculation algorithm for stereotactic and conventional lung volumetric modulated arc therapy plans. Radiat Oncol 2013;8:1. https://doi.org/10.1186/1748-717X-8-149.

[14] Yan C, Combine AG, Bednarz G, Lalonde RJ, Hu B, Dickens K, et al. Clinical implementation and evaluation of the Acuros dose calculation algorithm. J Appl Clin Med Phys 2017;18:195–209. https://doi.org/10.1002/acm2.12149.

[15] Tillikainen L, Helminen H, Torsti T, Siljamäki S, Alakuijala J, Pyyry J, et al. A 3D pencil-beam-based superposition algorithm for photon dose calculation in heterogeneous media. Phys Med Biol 2008;53:3821–39. https://doi.org/10.1088/0031-9155/53/14/008.

[16] Tillikainen L, Siljamäki S, Helminen H, Alakuijala J, Pyyry J. Determination of parameters for a multiple-source model of megavoltage photon beams using optimization methods. Phys Med Biol 2007;52:1441–67. https://doi.org/10.1088/0031-9155/52/5/015.

[17] Ma CM, Li J. Dose specification for radiation therapy: dose to water or dose to medium? Phys Med Biol 2011;56:3073–89. https://doi.org/10.1088/0031-9155/56/10/012.

[18] Andreo P. Dose to "water-like" media or dose to tissue in MV photons radiotherapy treatment planning: Still a matter of debate. Phys Med Biol 2015;60:309–37. https://doi.org/10.1088/0031-9155/60/1/309.

[19] Kan MWK, Leung LHT, Yu PKN. Dosimetric impact of using the acuros XB algorithm for intensity modulated radiation therapy and rapidarc planning in nasopharyngeal carcinomas. Int J Radiat Oncol Biol Phys 2013;85:e73–80. https://doi.org/10.1016/j.ijrobp.2012.08.031.

[20] Hirata K, Nakamura M, Yoshimura M, Mukumoto N, Nakata M, Ito H, et al. Dosimetric evaluation of the Acuros XB algorithm for a 4 MV photon beam in head and neck intensity-modulated radiation therapy. J Appl Clin Med Phys 2015;16:5222. https://doi.org/10.1120/jacmp.v16i4.5222.

[21] Kathirvel M, Subramanian S, Clivio A, Arun G, Fogliata A, Nicolini G, et al. Critical appraisal of the accuracy of Acuros-XB and Anisotropic Analytical Algorithm

compared to measurement and calculations with the compass system in the delivery of RapidArc clinical plans. Radiat Oncol 2013;8:1–9. https://doi.org/10.1186/1748-717X-8-140.
[22] Zifodya JM, Challens CHC, Hsieh WL. From AAA to Acuros XB-clinical implications of selecting either Acuros XB dose-to-water or dose-to-medium. Australas Phys Eng Sci Med 2016;39:431–9. https://doi.org/10.1007/s13246-016-0436-z.
[23] Varian Medical Systems. Eclipse algorithms reference guide for Eclipse version 10. 0. B502679R01B. Palo Alto, CA: Varian Medical Systems; 2010. n.d.
[24] Varian Medical Systems. Eclipse algorithms reference guide for Eclipse version 11. 0. B503486R01B. Palo Alto, CA: Varian Medical Systems; 2011. n.d.
[25] Vorwerk H, Hess CF. Guidelines for delineation of lymphatic clinical target volumes for high conformal radiotherapy: head and neck region. Radiat Oncol 2011;6:97. https://doi.org/10.1186/1748-717X-6-97.
[26] Setton J, Caria N, Romanyshyn J, Koutcher L, Wolden SL, Zelefsky MJ, et al. Intensity-modulated radiotherapy in the treatment of oropharyngeal cancer: an update of the memorial sloan-kettering cancer center experience. Int J Radiat Oncol Biol Phys 2012;82:291–8. https://doi.org/10.1016/j.ijrobp.2010.10.041.
[27] Bedi M, Firat S, Semenenko VA, Schultz C, Tripp P, Byhardt R, et al. Elective lymph node irradiation with intensity-modulated radiotherapy: Is conventional dose fractionation necessary? Int J Radiat Oncol Biol Phys 2012;83. https://doi.org/10.1016/j.ijrobp.2011.12.016.
[28] Grégoire V, Ang K, Budach W, Grau C, Hamoir M, Langendijk JA, et al. Delineation of the neck node levels for head and neck tumors: a 2013 update. DAHANCA, EORTC, HKNPCSG, NCIC CTG, NCRI, RTOG, TROG consensus guidelines. Radiother Oncol 2014;110:172–81. https://doi.org/10.1016/j.radonc.2013.10.010.
[29] Brouwer CL, Steenbakkers RJHM, Bourhis J, Budach W, Grau C, Grégoire V, et al. CT-based delineation of organs at risk in the head and neck region: DAHANCA, EORTC, GORTEC, HKNPCSG, NCIC CTG, NCRI, NRG Oncology and TROG consensus guidelines. Radiother Oncol 2015;117:83–90. https://doi.org/10.1016/j.radonc.2015.07.041.
[30] ICRU. ICRU 83 Prescribing, Recording, and Reporting Photon-Beam Intensity-Modulated Radiation Therapy (IMRT). vol. 10. 2010. doi: 10.1093/jicru/ndq025.
[31] Bentzen SM, Constine LS, Deasy JO, Eisbruch A, Jackson A, Marks LB, et al. Quantitative analyses of normal tissue effects in the clinic (QUANTEC): an introduction to the scientific issues. Int J Radiat Oncol Biol Phys 2010;76:S3–9. https://doi.org/10.1016/j.ijrobp.2009.09.040.
[32] Katsuta Y, Kadoya N, Fujita Y, Shimizu E, Matsunaga K, Matsushita H, et al. Clinical impact of dosimetric changes for volumetric modulated arc therapy in log file-based patient dose calculations. Phys Medica 2017;42:1–6. https://doi.org/10.1016/j.ejmp.2017.08.004.
[33] Cilla S, Meluccio D, Fidanzio A, Azario L, Ianiro A, Macchia G, et al. Initial clinical experience with Epid-based in-vivo dosimetry for VMAT treatments of head-and-neck tumors. Phys Medica 2016;32:52–8. https://doi.org/10.1016/j.ejmp.2015.09.007.
[34] Branchini M, Fiorino C, Dell'Oca I, Belli ML, Perna L, Di Muzio N, et al. Validation of a method for "dose of the day" calculation in head-neck tomotherapy by using planning ct-to-MVCT deformable image registration. Phys Medica 2017. https://doi.org/10.1016/j.ejmp.2017.05.070.
[35] Huang B, Wu L, Lin P, Chen C. Dose calculation of Acuros XB and Anisotropic Analytical Algorithm in lung stereotactic body radiotherapy treatment with flattening filter free beams and the potential role of calculation grid size. Radiat Oncol 2015;10:4–11. https://doi.org/10.1186/s13014-015-0357-0.